CONTINUOUSLY TUNABLE SILICON PHOTONIC MEMS 2 × 2 POWER COUPLER

Alain Y. Takabayashi[1], Hamed Sattari[1], Pierre Edinger[2], Peter Verheyen[3], Kristinn B. Gylfason[2], Wim Bogaerts[3,4] and Niels Quack[1]

[1]École Polytechnique Fédérale de Lausanne (EPFL), Lausanne, SWITZERLAND

[2]KTH Royal Institute of Technology, School of Electrical Engineering and Computer Sciences, Micro and Nanosystems, Stockholm, SWEDEN

[3]Interuniversity Microelectronics Centre (IMEC), Leuven, BELGIUM

[4]Ghent University-imec, Photonics Research Group, Department of Information Technology, Ghent, BELGIUM

ABSTRACT

The integration of MEMS transducers in photonic integrated circuits provides opportunities for high efficiency photonic modulation and dynamic routing on-chip. We here present an electrostatically actuated, silicon photonic MEMS 2 × 2 power coupler, fabricated in IMEC's iSiPP50G platform followed by a dedicated MEMS release sequence. The in-plane, mechanical tuning mechanism provides analog power coupling between waveguides in a small form factor. With our experimental demonstration of broad, > 30 nm optical bandwidth, high extinction ratio of > 27 dB, and a low actuation voltage of only 6 V, the coupler fulfills the requirements for large-scale integration in next generation reconfigurable PICs.

KEYWORDS

Microelectromechanical systems, photonic integrated circuits, silicon photonics, photonics, optical switch.

INTRODUCTION

The advent of the ubiquitous transistor roughly 70 years ago heralded a new paradigm in computational power and complexity: we had entered the aptly named "Silicon Age." From there, the trend became a continuous increase in the density of devices on a single chip, which was made possible by ever-increasing levels of integration. Highly advanced Application Specific Integrated Circuits (ASICs) now solve complex tasks in our computers, our phones, and our cars [1].

According to a white paper from Intel in 2016, the non-recurrent engineering costs, the IP licensing, and physical design of an ASIC can surpass $10 million, and this does not even include the fabrication [2]. A Field Programmable Gate Array (FPGA) on the other hand, while not as optimized for a particular function, is a generalized Integrated Circuit (IC) that is software-reconfigurable and hence more flexible and less expensive to develop and produce. These properties make an FPGA ideal for prototyping and small-scale deployments.

The field of silicon photonics shares many attributes of silicon electronics. In particular, because both silicon and its abundant and accessible oxide can be used to guide light on a chip, it is possible to take advantage of the technical prowess and tools developed over decades in the silicon semiconductor industry [3]. Like their electronic counterparts, Photonic Integrated Circuits (PICs) have become a mainstay in modern society, especially in the field of telecommunication. Furthermore, it has increasingly become evident, as it has been for ASICs, that PICs can potentially also benefit from generalizability and software-enabled reconfigurability. Not only is this approach expected to be more cost effective and accessible, but such programmable PICs have the potential to provide efficient solutions in quantum information processing and neuromorphic computing [4], [5].

Several tuning mechanisms exist for introducing reconfigurability to a PIC, such as the thermo-optic, opto-mechanic, plasma dispersion, and electro-optic effects, with the first three suitable for silicon [6]. There is, however, an additional mechanism for optical modulation in silicon and that is through Microelectromechanical Systems (MEMS). This electrical-mechanical-optical transduction mechanism uses electrostatic actuation, for example, to physically displace refractive media and thereby alter the effective index of waveguides.

The implementation of key functions such as optical switching and phase shifting by mechanical means has been demonstrated previously, using both in-plane and out-of-plane electrostatic actuation [7]–[10]. Currently, these devices are equivalent to "single" transistors and there are only a few larger scale demonstrations [11], [12]. To reach very large-scale integration, MEMS-tuning of photonic devices must be integrated within standard silicon photonics platforms. These technology platforms combine the precision and convenience of CMOS processing with a vast selection of high-performance library components, such as low-loss waveguides and high-speed modulators/detectors [13].

We here present an in-plane, electrostatically actuated 2×2 continuously tunable power coupler. The device has been fabricated in IMEC's iSiPP50G silicon photonics platform and released through custom post-processing at EPFL's Center of MicroNanoTechnology (CMi). Furthermore, the device is compact and exhibits broadband behavior as well as a high Extinction Ratio (ER), making it an overall competitive MEMS-enabled silicon photonic device.

OPERATING PRINCIPLE AND DESIGN

A three-dimensional schematic of our 2×2 analog coupler is shown in Figure 1. The device consists of three parts, a suspended, movable portion with a waveguide and attached comb drive; a suspended, fixed waveguide; and a fixed comb drive. All ports are anchored to a silicon rim (not pictured) through an optical transition indicated in the figure by a shallow-etched region rib waveguide. In the default state, i.e., with no voltage applied, the gap between the suspended waveguides in the coupling region is 150 nm, defined by lithography.

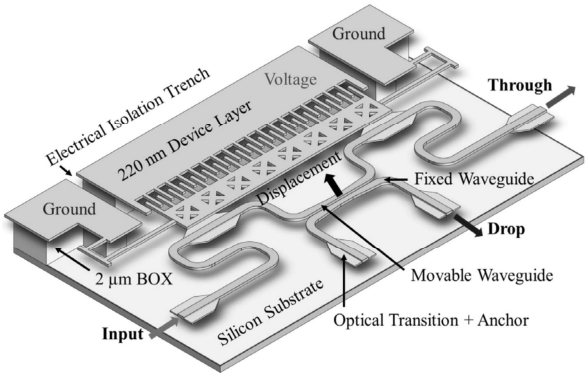

Figure 1: Schematic of the horizontally moving 2×2 analog coupler indicating Input and Drop/Through ports as well as the comb-drive actuator. Dimensions are not to scale.

This small gap separation ensures strong evanescent field coupling between the two such that light propagating in one waveguide will be transferred to the other.

In this default state, when light is injected into the *Input* port, most of the light is transferred to the *Drop* port. By grounding the movable electrode of the electrostatic comb drive and applying a voltage to the fixed electrode, an electrostatic force is generated that pulls the movable waveguide away from its fixed counterpart. In doing so, the gap between the two increases and coupling decreases. With a high enough voltage, the moveable waveguide is sufficiently far away from the fixed waveguide to allow all the optical power to propagate to the *Through* port. This method of operation is graphically depicted in Figure 2.

As indicated in Figure 2, the waveguides and comb drives are fabricated from the 220 nm thick device layer silicon, which in the anchored regions lies atop a 2 µm thick Buried Oxide (BOx) layer. The rib waveguides used in the optical transitions are etched 70 nm into the silicon and ensure low-loss transit through the silicon rim into the air-clad MEMS cavity.

The coupling region of the device is 30 µm long and contains symmetric tapering of the waveguide width from 450 nm to 300 nm, to reduce optical losses and increase optical bandwidth. Previous work reports on the detailed design by 3D Finite Difference Time Domain (FDTD) simulation to characterize the lateral gap versus transmission of in-plane moving devices and to predict an insertion loss of < 0.5 dB [14]. The device is designed to operate in the region where optical power in the *Drop* port is initially at a maximum for a gap of 150 nm. Power decreases to a minimum for a gap of approximately 200 nm and a coupling length of 30 µm, and because of the associated beat length, increases again for gaps beyond 200 nm, as schematically depicted in Figure 2.

The comb drives are able to provide the > 200 nm required displacement under an applied voltage of 13 V, which is compatible with standard driving electronics. In terms of footprint, the full device is 140 µm x 60 µm. Including the silicon rim and MEMS cavity used for electrical and optical input/output, the "unit cell" is 190 µm x 115 µm, which is compact and comparable to the dimensions of similarly demonstrated silicon photonic MEMS devices [9], [10].

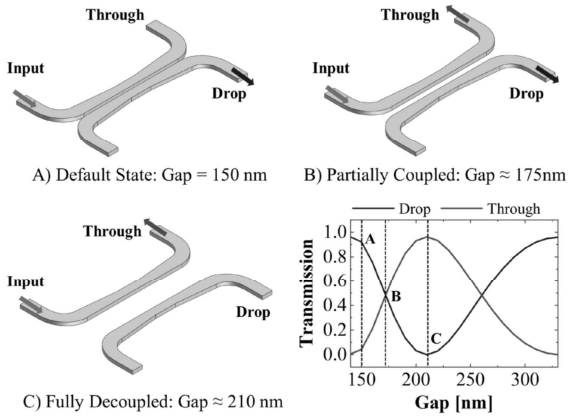

Figure 2: Visualization of the coupling region in the MEMS 2×2 analog power coupler, indicating how increasing the coupling gap affects optical transmission from Input to Through and Drop ports respectively.

FABRICATION

Design of this silicon photonic MEMS coupler takes place within the framework of IMEC's iSiPP50G platform and fabrication at IMEC occurs on 200 mm wafer-level scale. Following dicing into 2 x 2 coupons, i.e., four 23 mm x 23 mm chips, we perform a custom post-processing release procedure to release the device and make it free-standing. It should be noted that while the work presented here was performed on coupon- and chip-scale in order to enable short loop development cycles, all required process steps are entirely wafer-scale compatible.

MEMS are currently non-standard components in silicon photonic technology platforms. However, there is a standard etch in the iSiPP50G platform that removes portions of the back-end-of-line (BEOL) stack up to the Device Layer (DL) silicon. We use this etch step to define our MEMS cavities and subsequently design our devices in the DL silicon. The BOx, which normally is the lower oxide cladding, serves as a sacrificial layer that is locally removed selectively to make the DL silicon free-standing.

A characteristic cross-section of the samples immediately following fabrication at IMEC and the final post-processed view are shown in Figure 3a and Figure 3b, respectively. The first key step consists of an alumina passivation to protect regions of the chip, in particular the BEOL stack from attack by the Vapor-phase HF (VHF) used to remove the BOx. Following this deposition, the alumina undergoes patterning by direct laser writing lithography and timed etching by wet and dry etchants. The final step is the VHF release, which removes the BOx to undercut structures, allowing them to be suspended. Use of a vapor phase etchant allows us to reduce the risk of stiction-related collapse. A more complete discussion of the processing details can be found elsewhere [9].

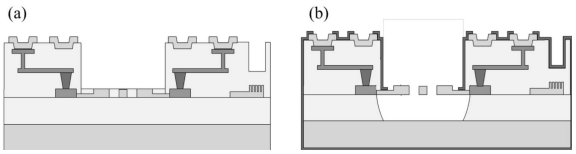

Figure 3: (a) Initial cross-section highlighting topography, metallization for electrical contact and sealing, and MEMS cavity opening in BEOL stack to DL silicon. (b) Final cross-section with alumina passivation and released device.

The optical microscope image in Figure 4a provides an overview image of the device alongside library-standard components, which include high-efficiency grating couplers, low-loss waveguides, and metallization for electrical routing and contacting. This particular release process does not make use of the sealing ring. However, it is possible to use this metallization in future work for a wafer-sealing process to encapsulate and protect the device from the ambient surroundings, a crucial step to ensure long term reliability of MEMS devices [15]. The SEM recording in Figure 4b provides a closer view of the coupler itself and its cleanly released (i.e., suspended) portions.

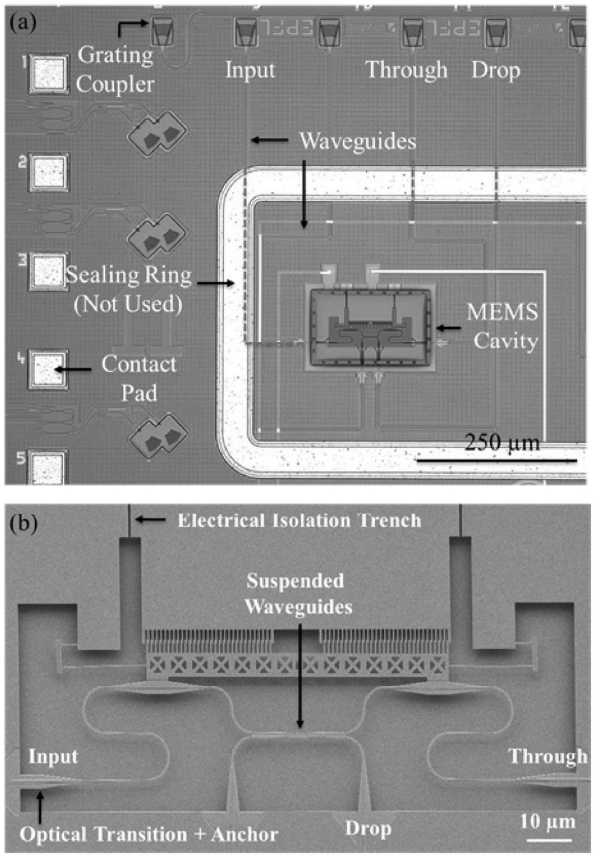

Figure 4: (a) Optical microscope image providing context for the device within the MEMS cavity alongside peripheral components including electrical and optical I/O. (b) SEM recording of the released 2×2 analog coupler, showing the suspended structures and electrical isolation trench and optical transitions/anchors.

RESULTS AND DISCUSSION

Characterization of the steady-state spectral response and power transmission as a function of applied voltage is performed using a tunable laser, fiber array, power detector module, and electrical probes connected to a DC power supply. An optical microscope image of the device under test with the salient components of the measurement setup is provided in Figure 5.

Light is injected into the PIC by means of connecting the tunable laser to a fiber array containing 10 fibers that have been aligned to the on-chip grating couplers. Waveguides then transfer the light into and out of the device, where it is coupled out of the PIC and into two separate power detector modules for measuring the transmission in the *Drop* and *Through* ports. Voltage is applied between the fingers of the comb drive via the DC power supply-connected electrical probe tips. One tip provides electrical grounding of the substrate to prevent out-of-plane displacement and the other two provide the voltage difference needed for electrostatic actuation.

The first set of measurement curves shown in Figure 6 illustrate the spectral behavior of this silicon photonic MEMS analog coupler for a series of applied voltages. In the initial state (actuation voltage 0 V, gap 150 nm), the device exhibits a 3 dB optical bandwidth of 30 nm in the *Through* port. This broadband behavior is maintained for each subsequent voltage up to the final 13 V.

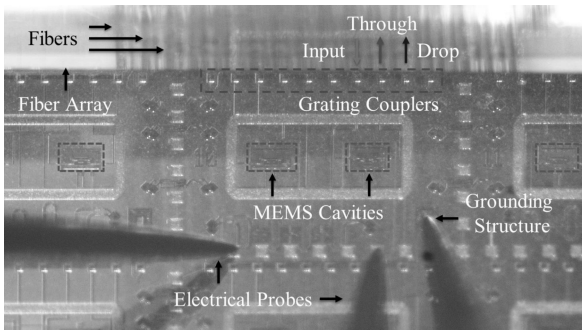

Figure 5: Characterization setup indicating the fiber array for optical input and output via the on-chip grating couplers and the electrical probes for applying voltage to the comb drives.

By focusing on a particular wavelength, e.g. the design wavelength of 1550 nm, it is possible to extract a power transmission versus applied voltage characteristic. In this case, the applied voltage can serve as a proxy for the gap used in Figure 2 because progressively larger voltages correspond to larger gaps. The results of this power vs. voltage sweep for 1550 nm are shown in Figure 7. As expected, in the initial state, where the coupling gap is small, we observe that the optical power is transferred preferentially to the *Drop* port.

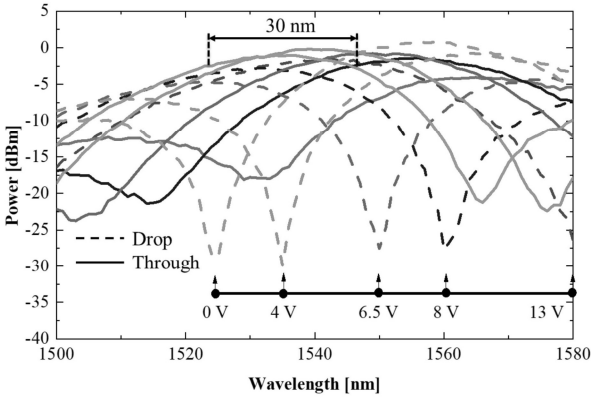

Figure 6: Spectral response of the analog coupler for a subset of applied voltages for 0 dBm input power. Power transmission has been normalized to the maximum measured power to remove the effects of misalignment, and losses in the grating couplers and measurement setup.

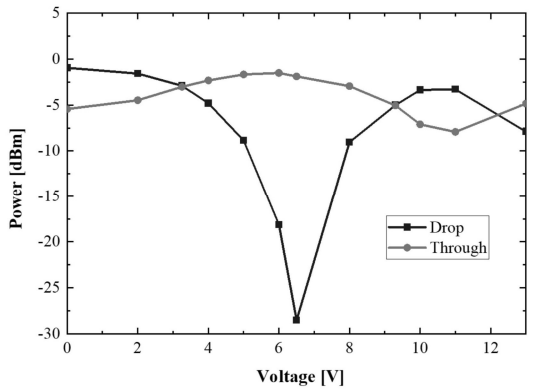

Figure 7: Transmitted power vs. actuation voltage for 1550 nm and an input power of 0 dBm.

However, the *Through* port also exhibits moderately high power transmission (i.e., 6 dB less than that seen in the *Drop* port), indicating incomplete coupling. Ideally, we should observe a characteristic more similar to that seen in state A of Figure 2 where there is a more distinct separation in power levels of the *Drop* and *Through* ports. This discrepancy can be explained by a misalignment of the suspended waveguides either in-plane, or out-of-plane. Geometric asymmetries, such as in the coupling region, e.g., a skew, rather than parallel, arrangement of waveguides, can lead to inefficient coupling. The asymmetric crab-leg suspensions in this particular implementation (Figure 4b) can further cause the electrostatic force, which pulls the movable waveguide away, to generate an undesirable torque that can rotate the device out of plane. Nevertheless, as the voltage increases, the effects of any geometric asymmetries or out-of-plane misalignment are reduced because the physical distance between waveguides increases. For roughly 6 V, we see that the gap has been made sufficiently large so as to completely transfer optical power to the *Through* port, with only residual power being coupled to the *Drop* port. In this state, the device exhibits an extinction ratio (ER) greater than 27 dB. Following the behavior predicted by simulation, further separation of the waveguides beyond 200 nm leads again to an increased power transmission to the *Through* port. While the insertion loss of the device is predicted < 0.5 dB by simulation [14], its experimental characterization has not been the focus of the presented study and dedicated test structures can be included in future work.

CONCLUSION

We have presented the design, fabrication, and characterization of a new type of in-plane, silicon photonic MEMS 2 × 2 continuously tunable power coupler. The use of adiabatic tapering in the coupling region allows the device to be broadband with > 30 nm of optical bandwidth. Tuning in the *Drop* port to a maximum ER > 27 dB at 6 V of actuation voltage has been achieved. Furthermore, by designing and fabricating a compact device (140 µm x 60 µm) that employs electrostatic actuation within the iSiPP50G platform, we have demonstrated the feasibility of a scalable, in-plane, electrical-mechanical-optical tuning mechanism for use in reconfigurable PICs.

ACKNOWLEDGEMENTS

This project has received funding from the European Union's Horizon 2020 research and innovation program under grant No. 780283 (MORPHIC – www.h2020morphic.eu). H. Sattari acknowledges funding from the Hasler Foundation under grant No. 17008, and Niels Quack from the Swiss National Science Foundation under grant No. 183717.

REFERENCES

[1] S. Liu, J. Tang, Z. Zhang, and J.-L. Gaudiot, "CAAD: Computer Architecture for Autonomous Driving," p. 7.

[2] S. Lim, "Expect a Breakthrough Advantage in Next-Generation FPGAs," p. 12, 2016.

[3] G. T. Reed, W. R. Headley, and C. E. J. Png, "Silicon photonics: the early years," in *Optoelectronic Integration on Silicon II*, Mar. 2005, vol. 5730, pp. 1–18, doi: 10.1117/12.596921.

[4] W. Bogaerts *et al.*, "Programmable photonic circuits," *Nature*, vol. 586, no. 7828, Art. no. 7828, Oct. 2020, doi: 10.1038/s41586-020-2764-0.

[5] S. Gyger *et al.*, "Reconfigurable photonics with on-chip single-photon detectors," *Nat. Commun.*, vol. 12, no. 1, p. 1408, Dec. 2021, doi: 10.1038/s41467-021-21624-3.

[6] C. Errando-Herranz, A. Y. Takabayashi, P. Edinger, H. Sattari, K. B. Gylfason, and N. Quack, "MEMS for Photonic Integrated Circuits," *IEEE J. Sel. Top. Quantum Electron.*, vol. 26, no. 2, pp. 1–16, Mar. 2020, doi: 10.1109/JSTQE.2019.2943384.

[7] T. Nagai and K. Hane, "Silicon photonic microelectromechanical switch using lateral adiabatic waveguide couplers," *Opt. Express*, vol. 26, no. 26, pp. 33906–33917, Dec. 2018, doi: 10.1364/OE.26.033906.

[8] Q. Qiao *et al.*, "Multifunctional mid-infrared photonic switch using a MEMS-based tunable waveguide coupler," *Opt. Lett.*, vol. 45, no. 19, pp. 5620–5623, Oct. 2020, doi: 10.1364/OL.400132.

[9] A. Y. Takabayashi *et al.*, "Broadband Compact Single-Pole Double-Throw Silicon Photonic MEMS Switch," *J. Microelectromechanical Syst.*, pp. 1–8, 2021, doi: 10.1109/JMEMS.2021.3060182.

[10] P. Edinger *et al.*, "Compact low loss MEMS phase shifters for scalable field-programmable silicon photonics," in *Conference on Lasers and Electro-Optics*, Washington, DC, 2020, p. SM3J.2, doi: 10.1364/CLEO_SI.2020.SM3J.2.

[11] S. Han, T. J. Seok, N. Quack, B.-W. Yoo, and M. C. Wu, "Large-scale silicon photonic switches with movable directional couplers," *Optica*, vol. 2, no. 4, pp. 370–375, Apr. 2015, doi: 10.1364/OPTICA.2.000370.

[12] T. J. Seok, N. Quack, S. Han, R. S. Muller, and M. C. Wu, "Highly Scalable Digital Silicon Photonic MEMS Switches," *J. Light. Technol.*, vol. 34, no. 2, pp. 365–371, Jan. 2016, doi: 10.1109/JLT.2015.2496321.

[13] A. Rahim, T. Spuesens, R. Baets, and W. Bogaerts, "Open-Access Silicon Photonics: Current Status and Emerging Initiatives," *Proc. IEEE*, vol. 106, no. 12, pp. 2313–2330, Dec. 2018, doi: 10.1109/JPROC.2018.2878686.

[14] H. Sattari *et al.*, "Compact broadband suspended silicon photonic directional coupler," *Opt. Lett.*, vol. 45, no. 11, pp. 2997–3000, Jun. 2020, doi: 10.1364/OL.394470.

[15] G. Jo *et al.*, "Wafer-level vacuum sealing for packaging of silicon photonic MEMS," in *Silicon Photonics XVI*, Mar. 2021, vol. 11691, p. 116910E, doi: 10.1117/12.2582975.

CONTACT

*A. Takabayashi, tel: +41 21 693 77 37;
alain.takabayashi@epfl.ch

Session 5B Q&A - Optical MEMS

Session Chair:
Frank Niklaus, KTH Royal Institute of Technology, SWEDEN

07:50 - 07:55

B5-5B1 **A ONE-INCH APERTURE PIEZOELECTRIC TUNABLE LENS WITH SMALL FOOTPRINT**
Hitesh G.B. Gowda, Tobias Gräf, and Ulrike Wallrabe
University of Freiburg, GERMANY

07:55 - 08:00

B5-5B2 **BI-AXIAL MAGNETICALLY ACTUATED TUNABLE PRISM**
Pascal M. Weber, Matthias C. Wapler, Florian Lemke, and Ulrike Wallrabe
University of Freiburg, GERMANY

08:00 - 08:05

B5-5B3 **CLOSED-LOOP CONTROL OF QUASI-STATIC SCANNING PZT MICROMIRRORS WITH EMBEDDED PIEZORESISTIVE SENSING AND SPURIOUS MODE REJECTION**
Paolo Frigerio[1], Luca Molinari[2], Andrea Barbieri[2], Roberto Carminati[2], Nicolò Boni[2], and Giacomo Langfelder[1]
[1]Politecnico di Milano, ITALY and [2]STMicroelectronics, ITALY

08:05 - 08:10

B5-5B4 **ACOUSTICALLY LEVITATED SPINNING OPTICAL SCANNER**
Takashi Sasaki and Kazuhiro Hane
Tohoku University, JAPAN

08:10 - 08:15

B5-5B5 **MODELLING AND EXPERIMENTAL VALIDATION OF PIEZOELECTRICALLY DRIVEN MICRO-LENS ACTUATOR**
Syed Mamun R Rasid[1], Aron Michael[2], Hemanshu Roy Pota[1], Ssu-Han Chen[2], and Chee Yee Kwok[2]
[1]University of New South Wales, Canberra, AUSTRALIA and
[2]University of New South Wales, Sydney, AUSTRALIA

08:15 - 08:20

B5-5B6 **CONTINUOUSLY TUNABLE SILICON PHOTONIC MEMS 2 × 2 POWER COUPLER**
Alain Y. Takabayashi[1], Hamed Sattari[1], Pierre Edinger[2], Peter Verheyen[3], Kristinn B. Gylfason[2], Wim Bogaerts[3,4], and Niels Quack[1]
[1]École Polytechnique Fédérale de Lausanne (EPFL), SWITZERLAND, [2]KTH Royal Institute of Technology, SWEDEN, [3]Interuniversity Microelectronics Centre (IMEC), BELGIUM, and
[4]Ghent University-IMEC, BELGIUM

Session 5C Q&A - PowerMEMS 2 - Thermo - Tribo - Electro - Magnetic

Session Chair:
Fei Wang, Southern University of Science and Technology, CHINA

07:50 - 07:55

B5-5C1 **A STRATEGY TO REDUCE AIR BREAKDOWN EFFECT AND BOOST OUTPUT ENERGY FOR CONTACT-SEPARATION MODE TRIBOELECTRIC NANOGENERATOR**
Zeyuan Cao, Yao Chu, Shiwen Wang, Zibo Wu, Rong Ding, and Xiongying Ye
Tsinghua University, CHINA

07:55 - 08:00

B5-5C2 **MAGNETICALLY EXCITED PIEZOELECTRIC ENERGY HARVESTER FOR MICROPOWER SUPPLY AND WAKEUP APPLICATIONS**
Björn Gojdka[1], Torben Dankwort[1], Marc A. Nowak[1], Mani T. Bodduluri[1], Minhaz Ahmed[1,2], Sven Grünzig[1], and Fabian Lofink[1]
[1]Fraunhofer Institute for Silicon Technology ISIT, GERMANY and [2]Furtwangen University, GERMANY

THE 21st INTERNATIONAL CONFERENCE ON
SOLID-STATE SENSORS, ACTUATORS AND MICROSYSTEMS

TRANSDUCERS 2021

ONLINE VIRTUAL CONFERENCE

ONLINE

FINAL PROGRAM

CONFERENCE CHAIRS

Jürgen Brugger
EPFL, SWITZERLAND

Amy Duwel
Draper Laboratory, USA

Yoshio Mita
University of Tokyo, JAPAN

All indicated times in the program are Greenwich Mean Time (GMT)/Universal Time Coordinated (UTC)

SPONSORED BY

TRF TRANSDUCER RESEARCH FOUNDATION
connecting big ideas and small tech

semi

MEMS & Sensors Industry Group®

TECHNICAL SPONSORS

IEEE

MEMS
IEEE MEMS TECHNICAL COMMUNITY